

Scaling Inline Static Mixers for Flocculation of Oil Sand Mature Fine Tailings

Alebachew Demoz

Natural Resources Canada, CanmetENERGY-Devon, One Oil Patch Drive, Devon, AB, Canada T9G 1A8

DOI 10.1002/aic.14958

Published online July 27, 2015 in Wiley Online Library (wileyonlinelibrary.com)

Operations to reclaim mature fine tailings (MFT) ponds involve flocculation using high-molecular-weight polymers, for which inline static mixers are suited. Three different commercial static mixers were utilized to determine mixing parameters corresponding to optimal dewatering performance of flocculated MFT. MFT was treated with polymer solution under different mixing conditions. The dewatering rates passed through a peak with increasing mean velocity, V and Reynolds number, Re of the fluid. The greater the number of mixer elements, the lower the V and Re at which the peak dewatering rate occurred. Mixing parameters such as G -value, residence time, and mixing energy dissipation rate of the most rapidly dewatering flocculated MFT were dependent on mixer type and setup. In contrast, peak dewatering rates converged when scaled with respect to specific mixing energy, E , demonstrating that E is a suitable scale-up parameter for inline static mixing to produce optimally dewatering MFT. © 2015 American Institute of Chemical Engineers AIChE J, 61: 4402–4411, 2015

Keywords: dewatering, flocculation, mixing energy, inline static mixer, oil sand tailings, scale-up

Introduction

The Athabasca oil sands of Alberta constitute the third-largest proven reserve of nonconventional crude oil in the world. The oil sand ore contains 9–13% w/w bitumen, which is extracted from the ore mainly by hot water processing.^{1,2} Oil sand deposits are also found in Venezuela, Utah, West Africa, and Russia. Mineral solids make up about 80–85% w/w of the oil sand ore, and are discharged as tailings in slurry form following extraction.^{1,3} About 15–30% (w/w) of the solid waste consists of fine particles smaller than 44 μm , largely comprised of clay minerals. The tailings are impounded in ponds for water recovery and containment. Some of the water from the tailings slurry collects at the top of the containment ponds and is recycled. Over a period of years, the fine solids form a persistent suspension known as mature fine tailings (MFT). Left on its own, the MFT would remain indefinitely as a gel-like suspension. Ongoing production from the oil sands increases the tailings volume and would require further expansion of tailings storage areas, thereby posing environmental, economic, and engineering challenges. The need to restore the tailing ponds areas to their original state as dry landscape is undisputed.

Restoration work starts with flocculation of the suspended fine solids to form larger and denser aggregates that settle out. Single chemicals or combinations of megadalton-sized macromolecule flocculants are being used in the treatment of MFT. A pretreatment step in which inorganic coagulants supplement the polymer action may also be used. After the completion of the flocculation treatment, the following three methods are

used by industry to handle the waste for final disposal: thin lift drying, centrifugation, and rim ditch dewatering. In the thin lift drying method, flocculated MFT is first deposited (sprayed) to about a 10-cm thickness across a large horizontally inclined (graded) surface area. Free water is captured mainly as overflow during deposition. Once this layer is sufficiently dry, another layer of similarly treated MFT is overlaid on top to undergo drying. Alternating steps of thin layer deposition and drying are thus used to recover large volumes of stored MFT from the tailings ponds. For the method to be practical, the turnaround time between successive deposition steps has to be sufficiently short.

A second method of processing MFT is by centrifugation utilizing a horizontal solid-bowl decanter centrifuge. This type of centrifuge is suited for the solid/liquid separation of flocculated MFT.⁴ Little or no separation can be achieved unless the MFT is flocculated. However, at sufficiently high bowl rotation speeds, the larger and denser flocs of chemically treated MFT migrate outwards from the center axis and onto the bowl wall while the liquid occupies the inner volume near the center axis of the centrifuge. Accumulation of the flocculated material at the bowl wall creates a mass of solids having a reduced water content, referred to as cake, and a watery inner core called centrate. The cake is scraped to one end of the centrifuge bowl by a concentric screw-scroll while the centrate overflows over a weir and exits the unit. Of the handful of available commercial tailings management technologies, separation by solid bowl decanter centrifugation produces the most highly dewatered fine tailings waste at the point of discharge. This separation results in a cake having a solids content of about 60% w/w.

The third method used by industry to process MFT is called rim ditch dewatering, also known as deep pit consolidation. In

Correspondence concerning this article should be addressed to A. Demoz at Alebachew.Demoz@NRCan-RNCan.gc.ca.

this method, flocculated MFT is pumped to a deep containment area or pit. As the treated MFT settles, some of the water makes its way to the surface through the pores of the large flocs, similar to what occurs during thin lift drying. The release water and rainfall runoff water are collected, either at low spots on the surface or via rim ditches constructed around the deposit. The rapid and continuous return of reclaimed water for recycle minimizes the potential for water losses and tends to accelerate consolidation of the deposit. The self-weight of the MFT in the pit consolidates the solids underneath, squeezing out more entrapped and interstitial water. All of these processes occur concurrently and their combined effects are expected to result in deposits sufficiently strong to bear loads for timely surface reclamation work.

The effectiveness of the three disposal methods described above is dependent on effective flocculation and, therefore, mixing. This study examines applications of inline static mixers for flocculation to produce optimally dewatering MFT. Inline static mixing, when feasible, has a number of operational and cost advantages. Static mixers are compact, low in cost, consume little power, and do not have moving parts that require maintenance or result in sealing problems. Inline static mixers are often used as single-pass mixers. There is no need to maintain an inventory of feed as the MFT can be treated on demand directly from the tailings pond. The material residence time is short and good mixing is achieved owing to near-plug-flow behavior. In contrast, the capital and operating costs of dynamic mixers capable of handling large inventories of MFT in a timely manner would be relatively high. All these factors make inline static mixers attractive as an MFT flocculation option.

Static mixers consist of specially designed rigid structures coupled end-to-end in pipes to enhance laminar and turbulent mixing. The mixing elements repeatedly split and recombine the mixture radially as the axial flow continues. This action achieves a mixture having uniform composition. Static mixer elements are broadly categorized into helical or twisted-ribbon, corrugated plate, and structured geometries (grids). Corrugated plate static mixers such as the Sulzer SMV™ feature highly constricted flow passages and are impractical for MFT flocculation. The Koflo and KMS static mixers used in this study have about 90% void volume and are better at coping with plugging and deposition (fouling) problems during flocculation. From the perspective of static mixer selection, high-pass static mixers with blades protruding from the wall, such as the Chemineer-Kenics HEV™ mixer, enhance avoidance of flow restrictions associated with accumulation of deposits from MFT.

Field observations and investigations of the dewatering rate of MFT flocculated using both static and dynamic mixers have shown that the dewatering rate of the flocculated solids is dependent on aspects of mixing, especially mixer type, mixing time, and mixing intensity.^{5–8} While static mixers are widely used in food processing; the manufacture of paints, polymers, and pharmaceuticals; and water treatment,^{9,10} the literature on their application in flocculation of oil sand MFT is limited. Management of oil sand MFT operations currently appears to rely on operator experience and some trial and error, an approach that is normally accompanied by start-up problems, downtime, and a lack of guidelines for restoring upset operations. This study is an attempt to provide operating guidelines by examining MFT flocculation and dewaterability performance using commercial static inline mixers. Dewatering

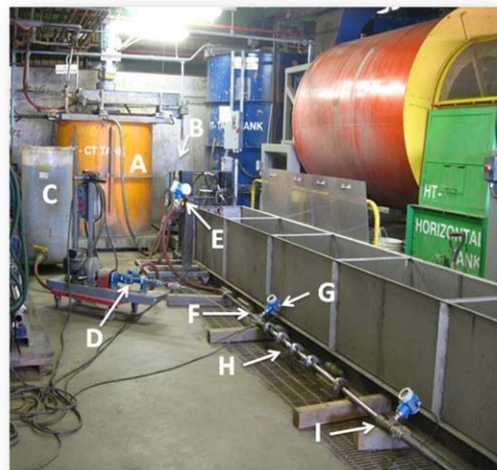


Figure 1. MFT flocculation test setup.

(A) MFT holding tank, (B) MFT pump, (C) polymer solution tank, (D) polymer pump, (E) flowmeter, (F) polymer injection point, (G) inlet pressure gauge, (H) static mixers, and (I) outlet pressure gauge. [Color figure can be viewed in the online issue, which is available at wileyonlinelibrary.com.]

performance was evaluated by capillary suction time (CST) and the settling rate of the water/mud interface.¹¹ The overall goal was to determine an index or mixing parameter that correlates well with optimally dewatering flocculated MFT. Such a mixing parameter could then be applied to optimize static mixer flocculation systems and as a scaling parameter.

Materials and Methods

Some of the mixing tests required as much as a drum of MFT for every 5 min of test run. The tests were conducted in a pilot plant equipped with process units and sumps adequately sized to handle the relatively large volumes of material, as shown in Figure 1. The MFT was fed from a 2.2-m³ tank using a progressive cavity pump (capacity of 45 L/min). To maintain uniformity, the feed in the tank was continuously stirred while mixing proceeded. Polymer flocculant solution was pumped using another smaller progressive cavity pump (capacity of 10 L/min). The volume of added polymer solution was varied in proportion with the MFT flow rate such that the experimental polymer dosage was held constant. The flow rates of the pumps were set using their own variable-frequency drives.

A high-molecular-weight (average molecular weight provided by the manufacturer of 18×10^6 g/mol), partially charged anionic polyacrylamide commercial macromolecule was used as flocculant. The flocculant dosage was 1100 g of dry polymer per ton of solids in the MFT. The feed was pre-conditioned with gypsum at a concentration of 1000 g per ton of MFT solids. The flocculant solution concentration was 0.1% (w/w). Flocculant solution was injected at the center line of a 1-inch diameter pipe, as close to the static mixer inlet as possible to ensure rapid mixing so that the flocculant would not drift to low-turbulence areas and stream out before being dispersed in the tailings.

Three different types of commercial stainless steel static mixers, depicted in Figure 2, were utilized in this mixing study: Chemineer-Kenics, KMS; Koflo 275; and Komax triple-action. The Koflo and Komax mixers were acquired as

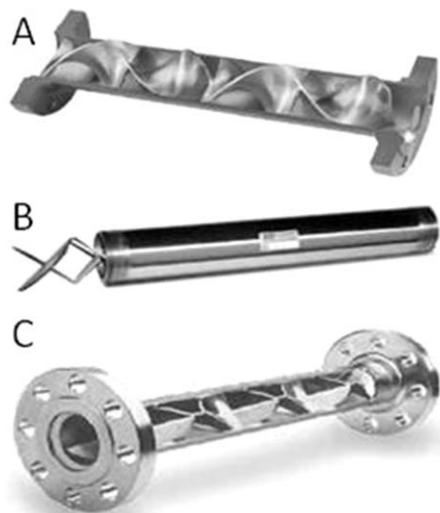


Figure 2. Cut-away views of inline static mixers used.

(A) Kenics-KMS, (B) Koflo 275, and (C) Komax triple-action mixer.

12-element units with 1-inch male national pipe thread connections. For the KMS-type mixers, 4- and 8-element units were combined to get the total number of static mixer elements used in the tests. The adjoining pipes were also 1-inch nominal diameter schedule 40 pipes.

An Andreas+HauserTM Coriolis, PromasI flowmeter was placed upstream of the polymer injection point to measure the MFT flow rate. The pressure drop across the static mixers was measured using Andreas+HauserTM Cerabar S PMC71 pressure gauges (see Figure 1). The flowmeter and pressure gauges all had 4–20 mA analog signal outputs. These signal outputs were digitized and recorded by a PC interfaced with an Instru-Net 100TM data acquisition system from Omega Engineering (Laval, Quebec, Canada). Pressures and flow rates were recorded every 4 s.

Low-magnification images of untreated MFT and flocculated MFT were obtained using a Carl Zeiss DiscoveryV20 stereo microscope equipped with a Carl Zeiss AxioCam high-resolution camera. The stereo microscope and the camera were controlled with AxioVision software.

As the underlying aim of this work was the production of more readily dewatering MFT, mixing performance was evaluated using dewaterability measures: CST and the initial settling rate of the mud/water interface. Samples for dewatering rate measurements were collected at the discharge point of the 1-inch pipe, and only after the mixing had proceeded long enough to ensure that the sample was representative. Measurements of the initial settling rate were done in 1-L graduated cylinders. Some of the product was transferred to five CST cells. The CST measurements were conducted using a Triton Electronics meter and type 319 single-radius cell heads 10 mm in diameter and Whatman #14 filter paper. At least three measurements were utilized to arrive at a CST value.

Particle-size distribution (PSD) was measured by sedigraph analysis¹² of the solids obtained after Dean–Stark extraction of the MFT.¹³ The clay quantity was determined by methylene blue titration.¹⁴ Rheological measurements were carried out at 25.0°C using an ARES-G2 rheometer (TA Instruments, New Castle, DE) equipped with Peltier plate temperature control. Sandblasted parallel plates (40-mm diameter, 1-mm gap) were used to perform dynamic oscillation measurements. For

steady-shear rheological measurements, the samples were placed in a 30-mm cup with a four-bladed 27.7-mm vane tool.

Results and Discussion

The PSD of the solids in the MFT is a determining factor in the rate of liquid/solid separation. The sedigraph measurements of the MFT (Figure 3) show that 60 and 98% (w/w) of the solids were smaller than 2 μm and 44 μm , respectively. These values are generally considered as the margins of the clay and fine particle sizes in oil sand mining. Methylene blue titration of the solids after Dean–Stark extraction at 12.7 MEq per 100 g solids also indicated that the MFT solids were very high in clay content. The flocculant molecules cause the fines and clay particles to form aggregates and flocs whose channels allow free water to pass through. The concentration of flocculant required to produce optimally dewatering MFT has to be adjusted in accordance with the feed solids properties. It was increased when treating a higher-solids-content MFT feed, and increased even further when the clay fraction in the MFT was high.

Flocs and aggregates comprised of fine particles are sensitive to shear.^{5,15–19} The mechanical energy input to the inline static mixing process is reflected by pressure drop. The rate of energy dissipation is related to the mixer geometry and the material properties of the fluid, MFT in this case. The viscosity of the MFT increased with polymer treatment and was affected by the mixing process (see Figure 4). The addition of flocculant resulted in a flocculated system having a higher viscosity than that of the untreated MFT. The steady-shear limiting viscosities at low and high shear rates of the flocculated MFT tended toward Newtonian behavior, with shear-thinning behavior in the intervening shear rate range. The cross model equation can satisfactorily fit these types of viscosity–shear rate dependencies.²⁰

The steady-shear viscosity plots also show that the flocculated material was not a stable single-structure substance, but changed with the mixing process as well. The mixing effect was more evident in the low-shear-rate-limit viscosities, before some of the network structures disintegrated due to shear during the rheological measurements. The low-shear

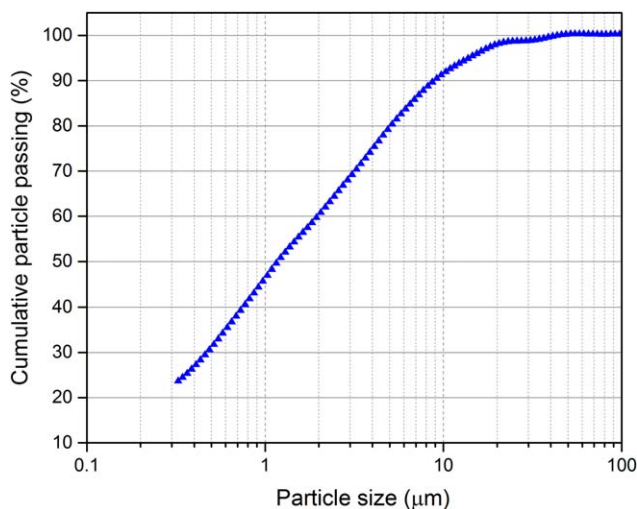


Figure 3. PSD of Dean–Stark extracted MFT solids by sedigraph.

[Color figure can be viewed in the online issue, which is available at wileyonlinelibrary.com.]

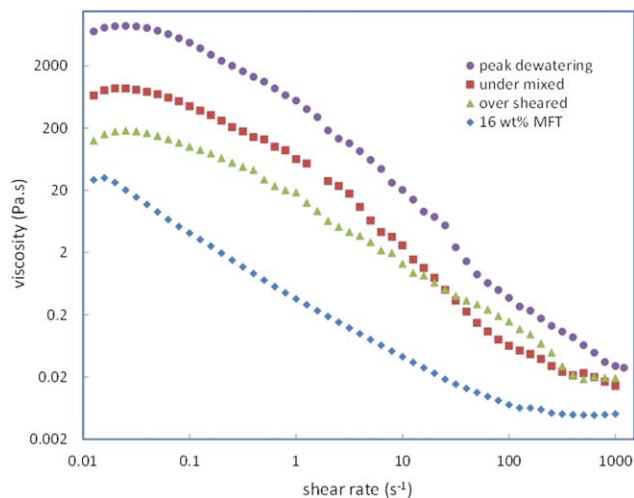


Figure 4. Progress of steady-shear viscosity of 16% (w/w) solids MFT as it was flocculated using the Komax inline static mixer.

The rheological measurements were conducted using a four-bladed vane and cup cell. [Color figure can be viewed in the online issue, which is available at wileyonlinelibrary.com.]

viscosity of the optimally dewatering inline flocculated material was higher than the viscosities of either the under- or over-mixed flocculated materials (see Figure 4). The macro-scale solids contents for all samples were the same. The observed viscosity differences reflected changes in the micro-scale network structures due to mixing.

The structural changes brought on by inline static mixing are also apparent from measurements of dynamic oscillation rheology. The addition of flocculant creates material whose complex modulus could be as much as three orders greater than that of the untreated MFT, as shown in Figure 5. Linear viscoelastic domain frequency sweep tests revealed that the loss and storage moduli were generally parallel in the frequency range from 0.02 to 625 rad s^{-1} , exhibiting the familiar characteristic of gel-like and networked dispersions.²⁰ Figure 5 also shows that the elastic modulus, G' , of the samples was higher than the viscous modulus, G'' , consistent with the formation of more-developed internal structures. As with the steady-shear rheological measurements, the complex modulus, G^* of the optimally dewatering flocculated MFT was higher than that of either the overmixed material or the untreated MFT. G' was progressively reduced for inline static mixings beyond the optimally dewatering flocculation. However, G' of the flocculated MFT remained greater than that of the untreated MFT, indicating that the over-mixing energy could rupture the extended network structures between flocs, but apparently was insufficient to render the flocs as dispersed solid particles as in MFT. The presence of primary aggregates that withstand extensive shearing and appear to network to form large flocs was also recorded in stereo micrographs as shown below. Strain-sweep measurements up to 200% are presented in Figure 6 for untreated MFT, optimally dewatering flocculated MFT, and this same sample after it was stirred with a spatula in a cup. The out-of-phase viscous response of untreated MFT began to show up from a strain amplitude of 0.12% while it was not noticeable until 8% for the flocculated MFT. The crossover from predominantly elastic to predominantly viscous behavior (see Figure 6) for MFT and floccu-

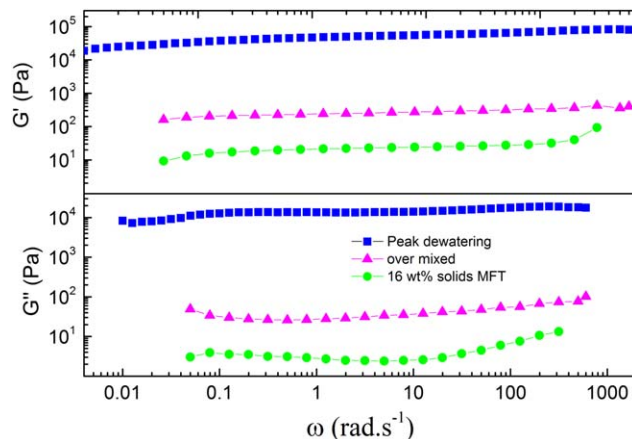


Figure 5. Dynamic moduli at 0.5% strain for MFT and flocculated MFT at two different mixing conditions.

[Color figure can be viewed in the online issue, which is available at wileyonlinelibrary.com.]

lated MFT occurred at strain amplitudes of 32% and 140%, respectively. All of these results indicate that the networked structure in the flocculated MFT is vulnerable to rupture when subjected to excessive mixing energy input. The optimally dewatering flocculation forms a highly networked structure and exhibits a more solid-like viscoelastic response as shown by the dynamic strain and frequency signal sweep results.

The stereo micrographs below show that individual polymer molecules gather several hundred fine solid particles forming flocs (Figure 7B). The micrograph of the optimally mixed MFT reveals that the flocculant bridges flocs together creating interlinked structures that incorporate large pores and channels. Water migrates upwards through these void spaces, resulting in the dewatering action. Further mixing beyond the optimal dewatering condition destroys the weaker bridging bonds, constricting the water release pathways. In agreement with the oscillatory dynamic rheological results, Figure 7C shows that the oversheared condition did not return the flocculated

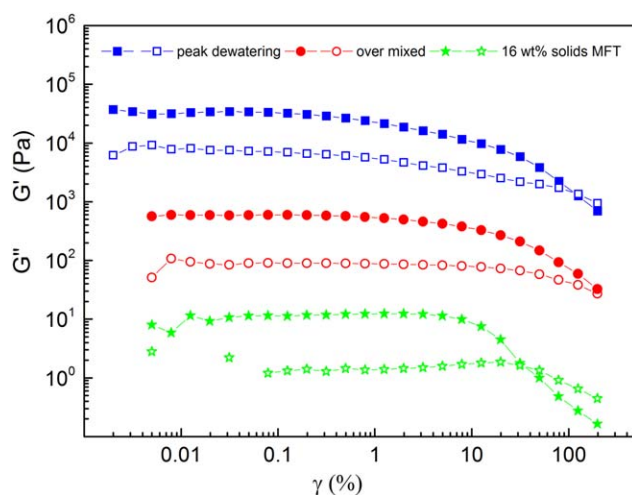


Figure 6. Strain amplitude sweeps at 10 rad s^{-1} of 16 wt % solids MFT and flocculated MFT.

Solid and open markers are for G' (elastic modulus) and G'' (viscous modulus), respectively. [Color figure can be viewed in the online issue, which is available at wileyonlinelibrary.com.]

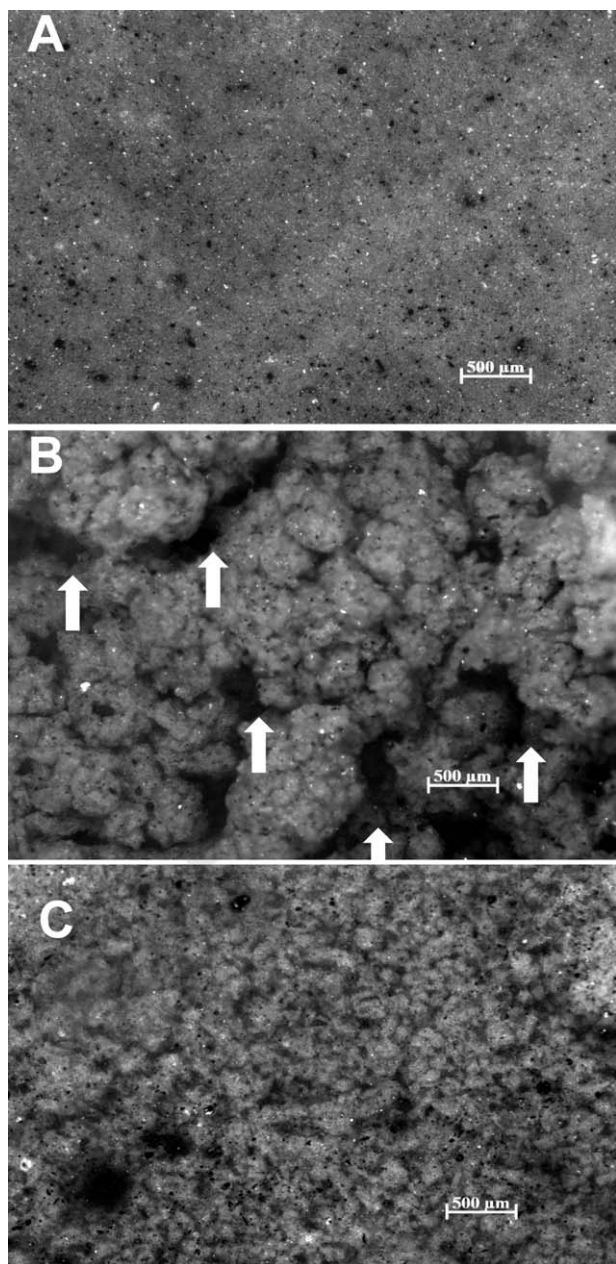


Figure 7. Stereo-micrographs obtained at the same magnification showing: A) untreated 21% (w/w) solids MFT; B) optimally mixed flocculated MFT; and C) same flocculated MFT as in B but oversheared. Arrows indicate free water channels.

solids to the original dispersed state of the untreated MFT. These results suggest that, in addition to the floc formation, the channel structures play a significant role in dewatering.

The measured pressure drops across the static mixers at various flow rates are given in Figure 8. MFT at 16% (w/w) solids exhibits Newtonian flow at high shear rates, as shown in Figure 4 (shear rate $> 100 \text{ s}^{-1}$). For the eight-element KMS mixer, more than one flow region can be distinguished based on the slope. In a laminar flow field, viscous forces dominate and the pressure drop has a linear dependence on flow rate. ΔP was nearly linearly dependent on flow rate for mean velocities corresponding to less than 5.32 L min^{-1} (or 0.2 m s^{-1}) in

open pipes. The flow through the eight-element KMS mixer was the only one that had a laminar zone (Figure 8). In turbulent flow regimes, the pressure drop is roughly a square function of velocity.²¹ The slope of the log–log plot of pressure drop vs. flow rate for greater numbers of elements of the KMS mixer was between 1.9 and 2. At all flow rates used, no similar breaks in the slopes were observed when using the Koflo and Komax static mixers, as illustrated by the Koflo pressure drop data in Figure 8. Moreover, the slopes of $\log \Delta P$ vs. $\log Q$ were close to 2, indicating that all of the flocculations using each of the static mixers were conducted under turbulent flow conditions.²¹

In laminar flow, the mixing proceeds by alternately splitting and remixing at the junction of elements and by sequential stretching and folding within the elements. In addition to the blending accomplished by such mixing, the material has to undergo sufficient hydrodynamic shear stress to form compact flocs. In turbulent flow, the elements intensify the turbulence by creating eddies of higher energy. This leads to more intense shearing and radial mixing, which, up to a point, are necessary to produce readily dewatering flocs. In all cases, the pressure drop across the static mixer increases linearly with the number of mixing elements. The dependence of pressure drop on the number of elements in static mixers is analogous to the dependence of pressure drop on pipe length in pipes. In fact, authors use the same pressure drop flow equation for static mixers as for open pipes^{22–24}

$$\Delta P = 2f \rho V^2 (L/D) \quad (1)$$

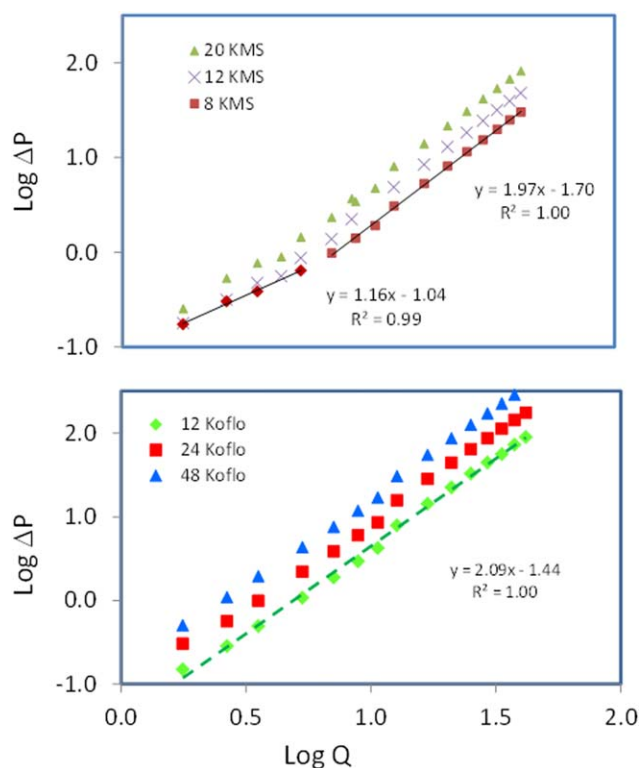


Figure 8. Empirical pressure drop across a series of KMS and Koflo static inline mixers for flow rates from $1.8\text{--}42 \text{ L min}^{-1}$ of 16% (w/w) solids MFT. Least-best-square regression lines and equations are shown.

[Color figure can be viewed in the online issue, which is available at wileyonlinelibrary.com.]

where f is the Fanning friction factor, V is the mean superficial velocity of fluid (m/s), ρ is the density (kg/m³), and D and L are the respective diameter and length of the static mixer (m). For static mixers, f additionally depends on the geometry and arrangement of the elements

$$f = g(\Delta P, D, L, V, \rho, \mu) \quad (2)$$

where μ is the apparent viscosity (Pa s, N s m⁻²). Application of the Buckingham π theorem dimensional analysis and combining friction terms into a constant characteristic for the specific static inline mixers simplifies Eq. 2 to²⁵

$$f = g(\text{Re}) \quad (3)$$

In the literature, f for static mixers is presented in two ways: first, as the ratio of the pressure drop across the static mixer to that across an open pipe of the same dimensions and, second, as empirical correlations based on measurements of flow rate and pressure drop across the static mixer. In the latter case, the empirical f is mathematically correlated with Re as implicitly put by Eq. 3. However, Re for systems whose properties are time-dependent is not definitive. Many of the $f(\text{Re})$ expressions in the literature are obtained by this approach.^{24,26}

The friction factor is an alternative way of expressing energy dissipation rate as given by Eq. 4. Figure 8 shows that the friction factor of a Koflo static mixer is higher than that of a KMS mixer at the same Re . Comparing the three commercial static mixers used in our studies, the friction factors of Koflo and Komax mixers are 1.85 and 2.3 times that of the KMS static mixer per element, respectively. This is in agreement with the general observation that static mixers with heli-coil surface elements show less pressure drop than those that utilize grids

$$f = \frac{\varepsilon D}{2V^3} \quad (4)$$

The dewatering rate of MFT flocculated using different impellers in stirred tanks was shown to pass through a peak with increasing mixing energy input. The specific energy dissipation for flocculation using dynamic mixing was shown to be the salient property determining the dewatering rates.⁷ It follows that other modes of flocculation, including inline static mixers, can have similar specific energy density dependence, as examined below. Kinetic energy supplied by the pump provides the mixing energy input for the inline static mixers. The specific energy dissipation rate across the static mixers, can be expressed as

$$\varepsilon = V \frac{\Delta P}{L} \frac{1}{\rho} \quad (5)$$

where ε is the specific energy dissipation rate per unit mass (W/kg). ε is related to the specific mixing energy dissipation, also referred to as the mixing energy density, by the equation below.

$$E = \varepsilon^* t \quad (6)$$

E is the specific mixing energy per unit mass (J/kg) and t is the mean residence time of the fluid in the static mixer (s). By examining two additional types of commercial static mixers we are extending the earlier conclusion inferred from the flocculation results for only the KMS static mixer, which showed that E associated with the mixing process for optimal dewatering can be used for scale-up of inline static mixing.⁸

The other often-mentioned flocculation parameters in oil sand tailings management are mean fluid velocity, V , and Re . Re is cited for almost any fluid flow process and, in this particular situation, may also indicate the mixing mechanism. These and other mixing parameters are well understood in a wide variety of applications, with the notable exception of oil sands MFT flocculation.⁹ In this work, we study these parameters, namely G -value, ε , E , Re , and V , and their relationships to optimally dewatering flocculated MFT.

For plug flow, the mean velocity for static mixers is obtained from Eq. 7. The static mixers used have comparable void ratios such that ignoring them would not affect our conclusions. The superficial velocity of the fluid reported in this article is therefore in reference to the nominal 1-inch diameter, schedule 40 pipe used in our tests.²⁷

$$V = \frac{4Q}{\pi D^2 \psi} \quad (7)$$

where ψ is the porosity of the static mixer, representing the void space.

There is ambiguity regarding the true shear rate in the choice of a suitable Re expression for non-Newtonian fluids. The Metzner–Reed Reynolds number, Re_g , is recognized as a generalized definition of Re ²⁸

$$\text{Re}_g = \frac{\rho D^{n'} V^{2n'}}{8^{n'-1} k'} \quad (8)$$

where k' and n' are the apparent consistency index and power index, respectively (different from the rheological power law model equation indices). The indices obtained by the usual manipulations of the nominal shear rate and wall shear stress were unrealistic because the n' values were greater than unity.^{28,29} This situation is in contradistinction to the fact that MFT and flocculated MFT are always shear thinning, that is, $n' < 1$ (see Figure 4).

Figure 4 shows that MFT and flocculated MFT have consistent viscosity at low and high shear rates. The rheology of the mixture is continually evolving from the moment the MFT and flocculant separately enter the static mixer to the time the mix leaves the static mixer. The floc sizes, size distribution, and viscosity are in flux during flow through the static mixers. A plausible approach supported by the vane shear rheological measurements (Figure 4) is to adopt pseudo-Newtonian viscosity at high shear as the apparent viscosity of the fluid flowing in the mixers. The steady-shear flow results obtained at high shear indicate that the apparent viscosities of all the flocculated MFTs tend to converge toward the same value. Consequently, Re is calculated using the conventional expression and the apparent viscosity μ obtained from the rotating rheological measurements

$$\text{Re} = \frac{\rho V D}{\mu} \quad (9)$$

The CST and initial mud/water interface measurement time scales are such that the former indicates the immediate dewatering rate (measurement time is often less than 3 min), while the latter indicates the short-term dewatering rate (a substantial fraction of the release water in the settling cylinders is collected in the first 30 min). The two measurements can be expected to agree as flocculated MFT starts dewatering without any induction period.³⁰ The use of CST and initial settling values are most appropriate for thin-lift operations, but

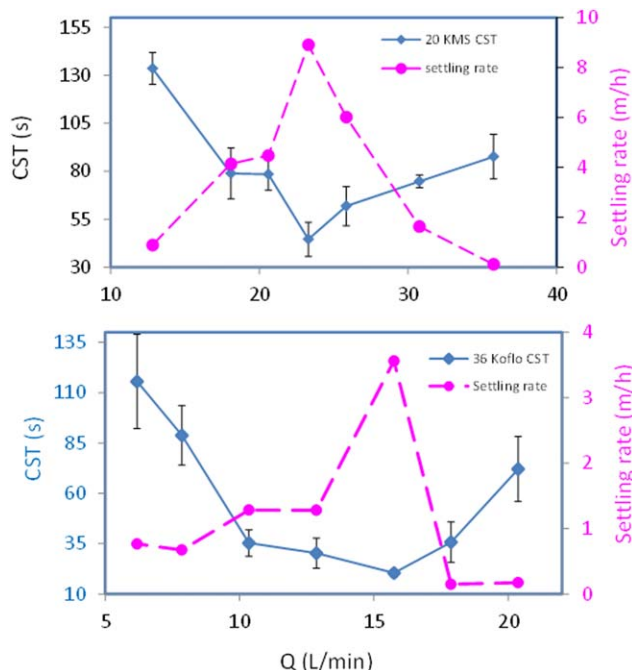


Figure 9. Flocculation evaluations by CST and initial settling rates of 20- and 36-element KMS and Koflo inline static mixers.

The error bars represent one standard deviation. [Color figure can be viewed in the online issue, which is available at wileyonlinelibrary.com.]

perhaps not as conclusive for deep-pit deposits where substantial time is acceptable for gravitational separation. As was the case in this study, the more readily the flocculated MFT dewaterers, the shorter the CST.¹¹ The flocculation that produced the peak settling rate also had the shortest CST in our study, as illustrated in Figure 9.

Figure 10 shows the initial settling rates of MFT flocculated using three types of static mixers, each incorporating two different numbers of mixer elements. It was consistently observed that the dewatering rate peaked and then decreased with increasing flow rate. The greater the number of mixing elements, the lower the flow rate for the given mixer at which the optimally dewatering flocculated MFT is produced. This means also that the residence time cannot be used as a criterion for optimally dewatering flocculation. Re dependence is a scaled version of V (flow rate) dependence (Eq. 9) as the flocculated MFT is considered to have a pseudo-Newtonian viscosity at the high experimental shear rates. Therefore, the same can be said of Re and its relationship to the peak dewatering rate. Greater numbers of mixer elements produce optimally dewatering flocculated MFT at lower Re compared to the same type of static mixer having fewer elements. The Re of the optimally dewatering flocculated MFT also varies with the mixer type.

The preferred mixer for a given application is normally presented by suppliers as the one having the lowest power demand. However, a static mixer so selected could turn out to be impractical due to factors such as plugging (likely with MFT) or a requirement for flow rates that are outside the workable ranges of other equipment or process requirements. In this study, different static mixers are considered, not for their power efficiency, but to determine scale-up parameters of the optimally dewatering flocculation utilizing inline static

mixers. Although, from an industrial perspective, the specific energy dissipation rate per unit mass, ε , is often evaluated to size pumps and address capital and operating costs, it is considered here as a scale-up parameter. For other processes analogous to flocculation, ε has also been employed to compare gas-liquid reactors and emulsion dispersion processes.^{31,32} Similar to V and Re , ε of the optimally dewatering

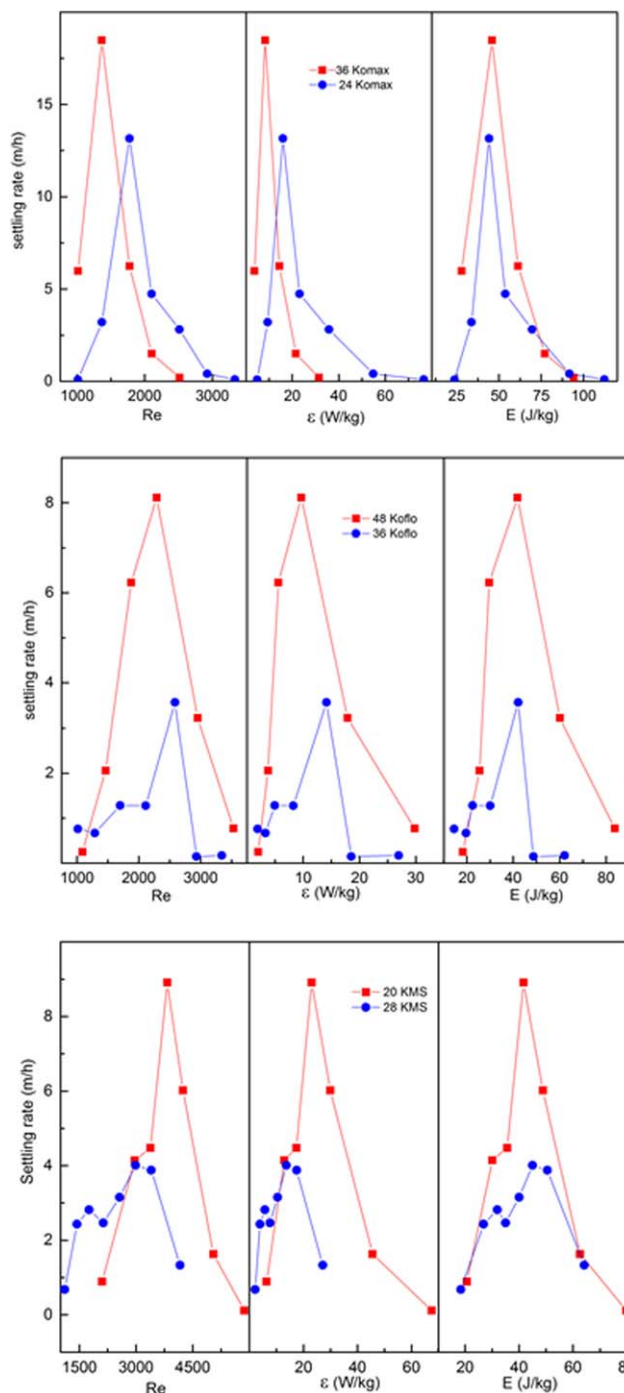


Figure 10. Initial settling rate relations with Re , ε , E of MFT flocculated using Komax, Koflo, and KMS static mixers.

Mixers having two different numbers of elements per type of inline static mixer are included. [Color figure can be viewed in the online issue, which is available at wileyonlinelibrary.com.]

Table 1. Properties Corresponding to the Optimally Dewatering MFT Flocculations Depicted in Figure 9

Mixer type	No.	η (μm)	t (s)	Re	G -value (1/s)	ε (W/kg)	E (J/kg)
KMS	20	47	1.8	3823	2177	23	42
	28	54	3.3	2984	1677	14	45
Koflo	36	53	3.0	2584	1707	14	42
	48	59	4.3	2289	1413	10	42
Komax	24	52	2.8	1776	1817	16	44
	36	61	5.5	1367	1310	8	46

flocculated MFT varies with the type of mixer and number of static mixer elements, as shown in Figure 10.

In the literature on water treatment and general environmental engineering, mixing is usually quantified using the velocity gradient (G -value). The G -value for static mixing is calculated from the energy loss as

$$G = \left(\frac{Q^* \Delta P}{\mu^* V_{\text{sm}}} \right)^{1/2} \quad (10)$$

where V_{sm} is the mixer volume (m^3).³³ It is now understood that there is no valid rationale for expecting that operations of equal G -value in stirred tanks, as in static mixing, should give the same mixing outcome.^{33,34} Nonetheless, the G -value still continues to be reported and is included in the table for the optimally dewatering flocculations. The spread of the values obtained for the optimally dewatering flocculations indicates that G -value cannot be used to correctly scale up flocculation of MFT using inline static mixers, in agreement with the wastewater studies of Amirtharajah's group³³ (and references cited within 33).

The velocity gradient impacts the dewatering rate in two ways. First, it is related to the turbulent shear patterns and turbulent eddy size. It is the redistribution of the hydrodynamic force that creates aggregates and flocs, and then breaks them when the stress exceeds their binding energy. While laminar flows have a single shear value, turbulent flows are characterized by a wide distribution of instantaneous and local shear rates. The prevailing understanding is that the hydrodynamic kinetic energy can be transferred whenever the eddies approach the size of the flocs, the former being defined by the Kolmogorov length scale^{35–37}

$$\eta = \sqrt{\frac{\mu}{\rho G}} \quad (11)$$

where η is the Kolmogorov's microscale of turbulence (m). Second, the velocity gradient empirically and semitheoretically has been considered related to aggregate size

$$d_{\text{eff}} = CG^{-m} \quad (12)$$

where d_{eff} is the effective floc diameter (m), m ($m > 0$) and C are constants, C scaling the floc strength.^{35–38} All of our inline static mixing tests were conducted at turbulent flow conditions. The released water did not contain residual polymer, showing that the distribution and interaction of the polymer with the slurry was complete. The d_{90} of the fines was less than 9 μm . The Kolmogorov lengths in these tests ranged between 35 and 90 μm . It is illustrated that the rupturing occurs on agglomerates similar in size to the eddies.^{35,36,38,39} Mixing at these cascading and fluctuating turbulent kinetic energy levels results in material exchange at the mesomixing scale. The implication of the shortest Kolmogorov dimensions being greater than four times the d_{90} of the MFT solids is that

smaller aggregates are subsumed in the eddies and unlikely to be ruptured.

The reduction in mixing time observed with increasing impeller rotation speeds to produce optimally dewatering flocculated MFT indicates that the process is controlled by the mixing energy per unit mass.⁷ Despite form differences, it is the same mechanical energy that drives the flocculation process in inline static mixers. For this reason, the specific mixing energy per unit mass, E , is examined as a scale-up parameter for flocculation by inline static mixers. E incorporates the effects of the mixer design, length, and flow rate. Figure 10 shows the settling rate dependencies with E for the three types of static mixers, each having two different numbers of mixer elements. The figure also makes it clear that, even though the tests were carried out at a limited number of flow rates, the optimally dewatering flocculated MFT was produced within approximately the same envelope of specific mixing energies, confirming our earlier preliminary findings on the subject.⁸ The mixing properties for the optimally dewatering tests are given in Table 1. Values of E are consistently similar in all of the mixing configurations; the small percentage variations are simply due to the limited number of tests. Table 1 also indicates that E is the property consistently correlated with the optimally dewatering mixing. These tests were conducted using single-diameter (1-inch nominal diameter) static mixers. However, the congruence of E across the radically different static mixer designs strongly suggests that E would also be valid for scaling mixer diameter. Along with E , the basic flocculation requirement of a minimum threshold of hydrodynamic stress required to form compact flocs also has to be met in the scale-up.

As much as mechanical agitation is needed to create large flocs it also can rupture them when the hydrodynamic stress exceeds the floc strength.^{35,38,40} Floc strength is dependent upon the interparticle bonds between the components of the aggregates.^{38,39} Bache et al.⁴¹ put forward a theoretical calculation method relating floc strength to hydrodynamic power and floc dimensions

$$\sigma = \frac{4\sqrt{3} \rho_w^2 \varepsilon^{3/4} d^{1/3}}{3 \mu^{1/4}} \quad (13)$$

where σ (N m^{-2}), is the average bond strength per unit area at the plane of rupture, ρ_w is the density of water (kg m^{-3}). The stability of flocs in the slurry is therefore dependent upon the number of the flocs and how readily they break, both of which are directly related to the mixing energy. The ε and G -value determine if the locally available kinetic energies are sufficient for flocculation and rupture. The specific energy input comprises these two intensive parameters as well as provide a measure of the balance between the formation and breakage of flocs and is, as demonstrated, the parameter that correlates well with the flocculation mixing for optimal dewatering. In the operational sense, E is directly related to the pressure drop,

which can be readily monitored by plant and field operators utilizing standard pressure gauges. The E -value required to achieve optimally dewatering flocculation can thus be maintained.

Conclusions

Inline static mixers are attractive for use in the large-throughput, continuous process required in the flocculation of MFT. Pilot-scale investigations of MFT flocculation by inline static mixing demonstrate that different styles of static mixers can be used to flocculate MFT. Multiple static mixer elements promote radial flow such that, starting from flow rates as low as 0.2 m s^{-1} , their flow is turbulent. Even with turbulent mixing, the flow rate has to be sufficiently high to achieve satisfactory flocculation.

1. For time-invariant fluid, the pressure drop is directly proportional to the number of elements for a given flow rate.

2. For a given inline mixer setup, the dewatering performance of flocculated MFT passes through a peak with increasing mixing conditions.

3. The greater the number of static mixer elements, the lower the flow rate at which peak dewatering performance is obtained.

4. The parameters ε , η , V , Re , t , and G -value were determined to be unsuitable for scaling with respect to achieving optimal dewatering of MFT flocculated by different static mixers.

5. The values of the specific mixing energy per unit mass, E , for the optimally dewatering flocculation by different types of inline static mixers is consistent. Similitude in the E of the optimal dewatering flocculation is therefore a sound basis for inline static mixer design and scale-up.

Acknowledgments

The author is thankful for support and funding for this project provided by the federal Panel on Energy Research and Development (PERD) under the ecoENERGY Innovation Initiative (ecoEII) program. All pilot plant tests were conducted with help from Craig McMullen and Dexter Woo. Vicente Munoz, acquired the stereo-micrograms. Vincent Castonguay from the Engineering faculty of the University of Alberta also participated as part of his student co-op training program. The author would like to thank Syncrude Canada Ltd. for providing MFT.

Notation

C = floc strength coefficient
 D = pipe diameter, m
 d_{eff} = effective diameter of flocs, m
 E = specific mixing energy per unit mass, J/kg
 f = Fanning friction factor, dimensionless
 G -value = velocity gradient, $1/\text{s}$
 G' = complex elastic modulus, Pa (N m^{-2})
 G^* = complex modulus, Pa (N m^{-2})
 G'' = complex viscous modulus, Pa (N m^{-2})
 k' = fluid consistency index, Pa s^n
 L = length of inline static mixer, m
 m = stable floc size exponent
 n' = apparent power index, dimensionless
 ΔP = pressure drop across static mixer, Pa (N m^{-2})
 Q = volumetric flow rate, $\text{m}^3 \text{ s}^{-1}$
 Re = pipe Reynolds number, dimensionless
 Re_g = Metzner-Reed Reynolds number, dimensionless
 t = mean residence time of fluid in inline static mixer, s
 V = mean fluid flow velocity in pipe, m s^{-1}
 V_{sm} = static mixer volume, m^3

Greek letters

ε = energy dissipation rate per unit mass, W/kg
 σ = average bond strength per unit area at the plane of rupture, N m^{-2}
 ρ = density of fluid, kg m^{-3}
 η = Kolmogorov length scale, m
 μ = fluid apparent viscosity, Pa s (N s m^{-2})
 γ = strain or deformation, dimensionless ($100\% = 1$)
 ψ = porosity of static mixer representing the void fraction
 ω = angular speed, rad s^{-1}

Literature Cited

- Gray M, Xu Z, Masliyah J. Physics in the oil sands of Alberta. *Phys Today*. 2009;62:31–35.
- Alberta Provincial Government, Alberta oil sands facts, 2014. Available at: www.energy.alberta.ca/oilsands/791.asp.
- Masliyah J, Zhou Z, Xu Z, Czarnecki J, Hamza HA. Understanding water-based bitumen extraction from Athabasca oil sands. *Can J Chem Eng*. 2004;82:625–864.
- Mikula RJ, Munoz VA, Omotoso O. Centrifugation options for production of dry stackable tailings in surface mined oil sands tailings management. *J Can Pet Technol*. 2009;48(Compendex):19–23.
- Hogg R. Flocculation and dewatering. *Int J Miner Process*. 2000;58:223–236.
- Gillis PA, Moore JS, Poindexter MK, Witham CA, Chen W, Singh H, Mohler CE, Atias JJ. The effects of in-line static mixer flow loop operational parameters on flocculant performance in mature fine tailings. *Tailings and Mine Waste '13*. Banff, AB, Canada, November 3–6, 2013:137–146.
- Demoz A, Mikula RJ. Role of mixing energy in the flocculation of mature fine tailings. *J Environ Eng ASCE*. 2012;138:129–136.
- Demoz A. Optimizing MFT dewatering by controlling polymer mixing. *3rd International Oil Sands Tailing Conference*. Edmonton, AB, Canada, December 3–5, 2012:141–147.
- Thakur RK, Vial CH, Nigam KDP, Nauman EB, Djelje G. Static mixers in the process industries. *Trans IChemE*. 2003;80:787–825.
- Etchells AW, Meyer CF. Mixing in pipelines. In: Paul EL, Atiemo-Obeng, Kresta SM, editors. *Handbook of Industrial Mixing*, Chapter 7. Hoboken: Wiley-Interscience, 2004.
- Scholz M. Revised capillary suction time (CST) test to reduce consumable costs and improve dewaterability interpretation. *J Chem Technol Biotechnol*. 2006;81:336–344.
- Jillavenkatesa A, Dapkuna SJ, Lum HL. *Particle Size Characterization, Recommended Practice Guide. NIST Special Publication 960-1*. Washington, DC: U.S. Government Office, 2001.
- Syncrude Research. *Determination of Bitumen, Water and Solids of Oil Sand, Reject and Slurry (Classical)*. Syncrude Research, Syncrude Canada, 1979.
- ASTM. Standard test method for methylene blue index of clay (C 837-99). *Annual Book of ASTM Standards, Sect. 15, Vol. 15.02*. Philadelphia, PA: American Society of Testing and Materials (ASTM), 1984.
- Heath AR, Bahri PA, Fawell PD, Farrow BJ. Polymer flocculation of calcite: experimental results from turbulent pipe flow. *AIChE J*. 2006;52:1284–1293.
- Rattanakawan C, Hogg R. Aggregate size distribution in flocculation. *Colloids Surf A*. 2001;177:87–98.
- Yeung AY, Gibbs A, Pelton R. The effect of shear on polymer-induced flocs. *J Colloid Interface Sci*. 1997;196:113–115.
- Sworska A, Laskowski JS, Cymerman G. Flocculation of the syncrude fine tailings: Part II. Effect of hydrodynamic conditions. *Int J Miner Process*. 2000;60:153–161.
- Owen AT, Fawell PD, Swift JD, Labbett DM, Benn FA, Farrow JB. Using turbulent pipe flow to study the factors affecting polymer-bridging flocculation of mineral systems. *Int J Mineral Process*. 2008;87:90–99.
- Tadros TF. *Rheology of Dispersions: Principles and Applications*. Weinheim, Germany: Wiley-VCH, 2010.
- Massey B, Ward-Smith J. *Mechanics of Fluids, 7th ed, Chapter 7*. Cheltenham, UK: Stanley Thorns Pub., 1998:197.
- Arzate A, Reglat O, Tanguy PA. Determination of in-line process viscosity using static mixers. *Flow Meas Instrum*. 2004;15:77–85.
- Liu S, Hrymak NA, Wood PE. Laminar mixing of shear thinning fluids in a SMA static mixer. *Chem Eng Sci*. 2006;61:1753–1759.
- Theron F, Sauze NL. Comparison between three static mixers for emulsion in turbulent flow. *Int J Multiphase Flow*. 2011;37:488–500.

25. Song H-S, Jan SP. A general correlation for pressure drop in a Kenics static mixer. *Chem Eng Sci.* 2005;60:5969–5704.
26. Kumar V, Shirke V, Nigam KDP. Performance of Kenics static mixer over a wide range of Reynolds numbers. *Chem Eng J.* 2008; 139:284–295.
27. Felicie T, Sauze LN, Ricard A. Turbulent liquid-liquid dispersion in Sulzer SMX mixer. *Ind Eng Chem Res.* 2010;49:623–632.
28. Chhabra RP, Richardson J. *Non-Newtonian Flow in the Process Industry.* Oxford: Butterworth-Heinemann, 2008.
29. Haldenwang H, Slatter PT, Chhabra RP. An experimental study of non-Newtonian fluid flow in rectangular flumes in laminar, transition and turbulent flow regimes. *J S Afr Inst Civ Eng.* 2010;52:11–19.
30. Jeeravpoolan S, Scott JD, Chalaturnyk RJ. 10m standpipe tests on oil sands tailings: long-term experimental results and prediction. *Can Geotech J.* 2009;46:875–888.
31. Heyouni A, Roustan M, D-Qaunag Z. Hydrodynamics and mass transfer in gas-liquid flow through static mixers. *Chem Eng Sci.* 2002;57:3325–3333.
32. Baumann A. *Deaeration of Fiber Suspension Using Tailored Dispersions Formed in Static Mixers*, PhD thesis. Swiss Federal Institute of Technology (ETH), Zurich, 2010.
33. Jones SC, Sotiropoulos F, Amirthrajah A. Numerical modeling of helical static mixers for water treatment. *J Environ Eng.* 2002;128: 431–440.
34. Graber SD. A critical review of the use of G-value (RMS velocity gradient) in environmental engineering. *Dev Theor Appl Mech.* 1994;17:533–556.
35. De Bona J, Lanotte SA, Vanni M. Internal stresses and breakup of rigid isostatic aggregates in homogeneous and isotropic turbulence. *J Fluid Mech.* 2014;775:365–396.
36. Bache DH, Floc rupture and turbulence: a framework for analysis. *Chem Eng Sci.* 2004;59:2521–2534.
37. Zacccone A, Soos M, Lattuada M, Wu H, Babler M, Morbidelli M. Breakup of dense colloidal aggregates under hydrodynamic stresses. *Phys Rev E.* 2009;79:061401.
38. Jarvis A, Jeffereson B, Gregory J, Parsons SA. A review of floc strength and breakage. *Water Res.* 2005;39:3121–3137.
39. Parker DS, Kaufmann WJ, Jenkins J. Floc breakup in turbulent flocculation processes. *J San Eng Div.* 1972;98:79–99.
40. Soos M, Kaufmann R, Winteler R, Kroupa M, Luthi MB. Determination of maximum turbulence energy dissipation rate generated by Rushton impeller through large eddy simulation. *AIChE J.* 2013; 59(10):3642–3658.
41. Bache DH, Rasool E, Moffatt D, McGilligan FJ. On the strength and character of alumino-humic flocs. *Water Sci Technol.* 1999;40: 81–88.

Manuscript received Feb. 4, 2015, and revision received June 3, 2015.